

How Powerful Potential of Attention on Image Restoration?

Cong Wang^{1,2}, Jinshan Pan³, Yeying Jin⁴, Liyan Wang⁵, Wei Wang¹, Gang Fu², Wenqi Ren¹, and Xiaochun Cao¹

¹ Sun Yat-sen University

² The Hong Kong Polytechnic University

³ Nanjing University of Science and Technology

⁴ National University of Singapore

⁵ Dalian University of Technology

Abstract. Transformers have demonstrated their effectiveness in image restoration tasks. Existing Transformer architectures typically comprise two essential components: multi-head self-attention and feed-forward network (FFN). The former captures long-range pixel dependencies, while the latter enables the model to learn complex patterns and relationships in the data. Previous studies have demonstrated that FFNs are key-value memories [17], which are vital in modern Transformer architectures. In this paper, we conduct an empirical study to explore the potential of attention mechanisms without using FFN and provide novel structures to demonstrate that removing FFN is flexible for image restoration. Specifically, we propose Continuous Scaling Attention (**CSAttn**), a method that computes attention continuously in three stages without using FFN. To achieve competitive performance, we propose a series of key components within the attention. Our designs provide a closer look at the attention mechanism and reveal that some simple operations can significantly affect the model performance. We apply our **CSAttn** to several image restoration tasks and show that our model can outperform CNN-based and Transformer-based image restoration approaches.

Keywords: Continuous Scaling Attention · Image Restoration · Derain-ing · Desnowing · Dehazing · Low-light Enhancement

1 Introduction

Image restoration aims to recover clear images from the given degraded ones. Reconstructing high-quality images benefits many practical applications, such as video surveillance, and self-driving techniques. This task is highly ill-posed as only degraded images are known while many solutions can correspond to the original ones. Early studies always apply statistic priors to make the problems well-posed [22, 26, 47, 49]. Although these prior-driven approaches can achieve clear results to some extent, they usually involve solving optimization problems that suffer from non-convexity issues and are time-consuming.

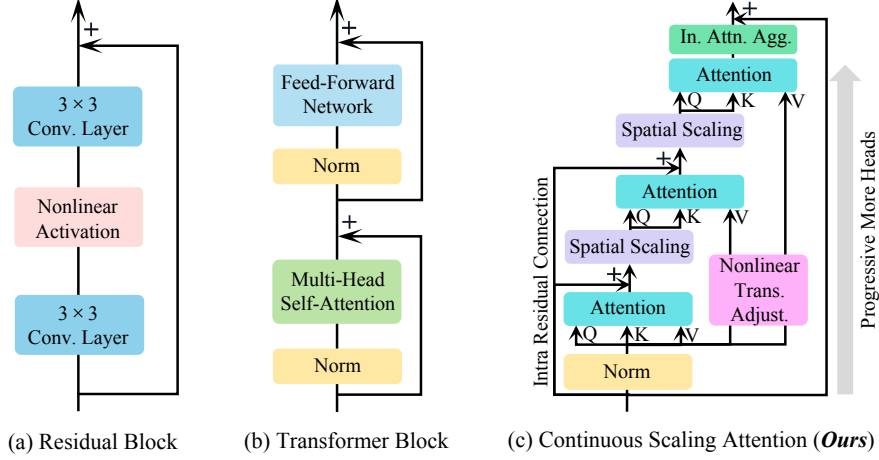


Fig. 1: Comparisons on Different Modern Blocks. (a) Residual block or its varieties are used to build the CNN-based image restoration methods [31, 77]. (b) Transformer block that usually contains multi-head self-attention and a feed-forward network provide the basic for Transformer-based image restoration approaches [37, 71]. (c) The proposed continuous scaling attention block. Different from CNN-based and Transformer-based blocks, we propose a Continuous Scaling Attention (**CSAttn**) block to explore how powerful potential of attention is *without using feed-forward network*, which is essential in existing Transformers [29, 55, 63, 71]. We demonstrate that by inserting several key designs into continuous attention, the attention is able to achieve competitive performance compared with CNN-based and Transformer-based approaches.

With the great success of convolutional neural networks (CNNs) [23, 30, 54], CNNs have been applied to many vision tasks and achieved remarkable performance. CNNs have also been explored in image restoration [33, 40, 52, 60–62], and outperformed previous prior-based methods. These CNN-based approaches are usually built on the residual block [23] or its varieties [25, 77], as shown in Fig. 1(a). Due to convolution being computed in local windows and exhibiting translation equivariance, the CNN-based approaches with limited receptive field prevent it from modeling long-range pixel dependencies.

Transformers [13, 28] calculate the response at a given pixel by a weighted sum of all other positions instead of using local receptive windows. They have been successfully applied to image restoration tasks and achieved impressive performance [6, 20, 58, 63]. In Fig. 1(b), existing Transformer frameworks usually involve two key designs: multi-head self-attention and feed-forward network (FFN). The former is used to perceive the long-range pixel dependencies while the latter is used for nonlinear transformation and enhancement of the features from attention. Moreover, some studies suggest that FFNs are essential and serve as the key-value memories [17]. While all the Transformers use the FFN, we would like to raise a challenge: is it flexible to use only the attention in Transformers without using FFN? *If so, how do we design the attention*

to ensure that it has powerful abilities compared with original Transformer blocks?

In this paper, we conduct an empirical study to explore the potential of attention on image restoration. Different from existing Transformer blocks that contain FFN after the attention computation, we propose Continuous Scaling Attention (CSAttn) which contains three attention *without using FFN* by introducing several key designs. **First**, instead of simply stacking 3 attention blocks, we propose Continuous Attention Learning to scale up model performance with a series of effective designs, which will be detailedly introduced below. **Second**, different from existing attention [41, 71] which usually does not contain the Nonlinear Activation function in attention modeling, we insert the Nonlinear Activation function into attention to activate more useful features. **Third**, we also suggest a *Value* Nonlinear Transformation Adjustment to adaptively adjust the *Value* features to produce more representative information to participate in the second and third attention computation. **Forth**, we introduce the Intra Attention Aggregation to fuse attention features to learn better attention representation from different levels. **Fifth**, we introduce Intra Progressive More Heads into these attentions to implicitly improve the attention representations. **Sixth**, we suggest the Intra Residual Connections to provide more useful features into the next attention computation so that better improves restoration quality. **At last**, we propose Spatial Scaling Learning to save the training budget while keeping the superior performance compared with the model without using scaling. By integrating these key designs into one entity, CSAttn is able to achieve superior performance compared with CNN-based and Transformer-based image restoration approaches. Fig. 1(c) shows the sketch of our CSAttn.

The main contributions are summarized below:

- We propose a Continuous Scaling Attention (**CSAttn**) block to explore the potential of attention without using FFN to empower attention with strong learning ability by designing a series of key components.
- We analyze and show how each part affects the final restoration performance to deliver deeper insights into our proposed CSAttn.
- We conduct extensive experiments to demonstrate that our CSAttn favors against state-of-the-art CNN-based and Transformer-based approaches on image restoration tasks including image deraining, image desnowing, low-light image enhancement, and real image dehazing.

2 Related Work

As discussed above, current image restoration techniques can be driven by convolutional neural networks and Transformers.

2.1 CNN-based Image Restoration

With the great success of deep learning on various vision tasks, CNNs also achieve remarkable performance on image restoration [10, 14, 72, 73, 80] due to powerful ability of implicitly learning the priors from large-scale data. Zhang *et*

al. [76] propose a CNN-based framework to solve the image denoising problem. Instead of directly learning the latent clear noise-free images, they devise a residual learning method to learn the noise, which achieves impressive performance compared to all previous optimization-based denoising approaches. Pan *et al.* [48] suggest a dual convolutional network for low-level vision, where they formulate the convolutional networks within the task-specific formulation. Ledig *et al.* [32] explore the generative generative adversarial networks [19] into image super-resolution for realistic quality. Cho *et al.* [9] rethink the image deblurring task from the coarse-to-fine mechanism, where they restore the latent clear images from coarser scales to finer scales. Zamir *et al.* [73] present a multi-stage progressive image restoration network, where they gradually recover the latent clear images from the perspective of multi-patches to entire images. In [11], Cui *et al.* propose a CNN-based selective frequency approach for image restoration and achieve impressive performance. We refer the readers to recent excellent literature reviews on image restoration [3, 35], which summarise the main designs in deep image restoration models.

2.2 Transformer-based Image Restoration

With the attention design of Transformers [13, 28] which calculates responses at a given pixel by a weighted sum of all other positions instead of local receptive windows, Transformers-based approaches have been successfully applied to image restoration tasks and achieved impressive performance [6, 20, 63]. Liang *et al.* [37] develop an Swin Transformer [41] framework for image restoration. They advance previous CNN-based image restoration approaches on various applications. Guo *et al.* [20] suggest a Transformer with transmission-aware 3D position embedding for image dehazing, where transmission implies the haze density that can provide the relative position information and haze density information to improve dehazing performance. Zamir *et al.* [71] introduce a Restormer to solving high-resolution image restoration problems, where they compute cross-covariance across feature channels to avoid quadratic computational complexity. Kong *et al.* [29] propose a frequency domain-based Transformer for image deblurring, where they integrate the frequency knowledge by Fast Fourier Transformation into Transformer architecture, effectively improving the deblurring results.

Different from existing Transformer architectures which usually use FFN after the attention, we propose continuous scaling attention without using FFN and achieve competitive performance on image restoration tasks by empirically designing a series of simple and effective techniques.

3 Proposed Approach

Our goal aims to explore how powerful potential of attention on image restoration and enhancement without using a feed-forward network (FFN) which is essential in existing Transformers [55, 63, 71]. To that end, we develop the new Continuous Scaling Attention (**CSAttn**), as shown in Fig. 2. Our CSAttn contains continuous three attentions without FFN. To scale up the attention capacity, we

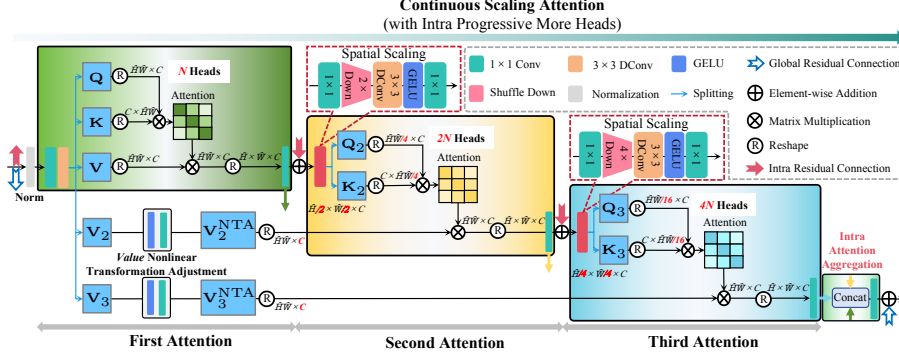


Fig. 2: Detailed structure of our Continuous Scaling Attention (CSAttn). Our CSAttn contains three continuous attention *without using FFN* which is essential in modern Transformer architectures [13, 63, 71]. By integrating a series of simple and effective designs into one entity, CSAttn is able to achieve competitive performance compared with CNN-based and Transformer-based image restoration approaches.

introduce a series of key designs, including (a) Continuous Attention Learning; (b) Nonlinear Activation function; (c) *Value Nonlinear Transformation Adjustment*; (d) Intra Attention Aggregation; (e) Intra Progressive More Heads; (f) Intra Residual Connections; (g) Spatial Scaling Learning. Next, we will formulate our proposed CSAttn and detailedly introduce the effect of each component.

3.1 Overall pipeline

Our overall network is the same as the network structure of SFNet [11], which is a three-level encoder and decoder framework with multiple inputs and multiple outputs. We replace the residual blocks in SFNet [11] with our proposed CSAttn blocks and adjust the number of blocks. We first input 1-scale, 1/2-scale, and 1/4 scale input images to 1-3 level encoder and then reconstruct the 1-scale, 1/2-scale, and 1/4 scale output results by decoder. We use the L_1 loss and frequency loss [9] to constrain these three outputs with default parameters in [11].

3.2 Continuous Scaling Attention

Our proposed Continuous Scaling Attention (CSAttn) is illustrated in Fig. 2, which contains three continuous attention computations with spatial scaling. At the first attention, our CSAttn is the same as the attention in Restormer [71]. In the second and third attention computations, instead of stacking the same attention with the first one which may be less effective, we propose a series of simple and effective techniques to scale up the attention capacity for better model performance.

Specifically, our first attention in CSAttn can be formulated as follows:

$$\begin{aligned} \mathbf{Q}, \mathbf{K}, \mathbf{V}, \mathbf{V}_2, \mathbf{V}_3 &= \text{Split}\left(W_d W_p(\hat{\mathbf{X}})\right), \\ \mathbf{X}_{\text{first}} &= \text{Attention}\left(\mathbf{Q}, \mathbf{K}, \mathbf{V}\right), \end{aligned} \quad (1)$$

where $\text{Attention}(\mathbf{Q}, \mathbf{K}, \mathbf{V}) = \mathbf{V} \cdot \text{Softmax}(\mathbf{K} \cdot \mathbf{Q} / \alpha)$; Here, α is a learnable scaling parameter to control the magnitude of the dot product of \mathbf{K} and \mathbf{Q} ; $\text{Split}(\cdot)$ denotes the split operation; $W_p(\cdot)$ refers to the 1×1 point-wise convolution, while $W_d(\cdot)$ means the 3×3 depth-wise convolution. We use N heads in the first attention; \mathbf{V}_2 and \mathbf{V}_3 denote the *Values* which will participate in the computation of the second and third attention; $\hat{\mathbf{X}}$ denotes the input features which are first normalized by layer normalization [4].

After conducting the first attention, we then compute the second and third attention. These two attentions have similar processes with several key techniques but are different from the first attention. The second attention, which contains three key techniques, including *Value Nonlinear Transformation Adjustment*, *Spatial Scaling*, and *Intra Residual Connection*:

$$\begin{aligned} \mathbf{V}_2^{\text{NTA}} &= \text{NTA}(\mathbf{V}_2), \\ \mathbf{Q}_2, \mathbf{K}_2 &= \text{Split}\left(\text{Scaling}\left(\mathbf{X}_{\text{first}} \oplus \hat{\mathbf{X}}\right)\right), \\ \mathbf{X}_{\text{second}} &= \text{Attention}\left(\mathbf{Q}_2, \mathbf{K}_2, \mathbf{V}_2^{\text{NTA}}\right), \end{aligned} \quad (2)$$

where **NTA** denotes the *Value Nonlinear Transformation Adjustment* operation, which contains a simple 1×1 convolution followed with a nonlinear activation function; **Scaling** means the spatial scaling operation, which contains 1×1 point-wise convolution, shuffle down operation, 3×3 depth-wise convolution, nonlinear activation function, and 1×1 point-wise convolution, where we use $2 \times$ shuffle down in the second attention; \oplus refers to the intra residual connection by adding to the original input $\hat{\mathbf{X}}$. Note that we use $2N$ heads in the second attention.

The third attention has similar processes to the second one:

$$\begin{aligned} \mathbf{V}_3^{\text{NTA}} &= \text{NTA}(\mathbf{V}_3), \\ \mathbf{Q}_3, \mathbf{K}_3 &= \text{Split}\left(\text{Scaling}\left(\mathbf{X}_{\text{second}} \oplus \hat{\mathbf{X}}\right)\right), \\ \mathbf{X}_{\text{third}} &= \text{Attention}\left(\mathbf{Q}_3, \mathbf{K}_3, \mathbf{V}_3^{\text{NTA}}\right), \end{aligned} \quad (3)$$

where we use $4 \times$ shuffle down in the **Scaling** operation and $2N$ heads in the third attention.

Last, we aggregate these three attention outputs to learn more representative features by concatenation and 1×1 point-wise convolution, which is further added to original input $\hat{\mathbf{X}}$:

$$\mathbf{Y} = W_p\left(\text{Concat}\left[\mathbf{X}_{\text{first}}, \mathbf{X}_{\text{second}}, \mathbf{X}_{\text{third}}\right]\right) + \hat{\mathbf{X}}, \quad (4)$$

where \mathbf{Y} means the output of CSAttn block; $\text{Concat}[\cdot]$ denotes the concatenation operation at channel dimension; $+$ means the global residual connections in the block.

3.3 Discussion on Continuous Scaling Attention

Our CSAttn involves a series of key designs. Discussing them to better explain our model is necessary.

(a) Continuous Attention Learning. As one single attention without FFN does not work well [17], we introduce a continuous attention mechanism to scale up attention capacity. Instead of directly stacking three attention, we propose the Continuous Scaling Attention with a series of key designs that are essential to model performance. We will demonstrate that these components will significantly benefit model capacity.

(b) Spatial Scaling Learning. We propose spatial scaling learning to save the training budget while keeping superior performance compared with the model without using scaling. The Spatial Scaling Learning contains 1×1 point-wise convolution, shuffle down operation, 3×3 depth-wise convolution, nonlinear activation function, and 1×1 point-wise convolution, where the shuffle down operation is used to reduce the spatial sizes. In the second attention, we use $2 \times$ shuffle down to reduce the size of the original input to $1/2$ scale, while we use $4 \times$ shuffle down to reduce the size of original input to $1/4$ scale in the third attention to efficiently compute these attentions.

(c) Value Nonlinear Transformation Adjustment. *Value* Nonlinear Transformation Adjustment is an essential operation, which involves very simple operations including 1×1 convolution and nonlinear activation, which aims to adaptively adjust the *Value* features to activate more representative content to effectively participate in the second and third attention computation.

(d) Nonlinear Activation Function. The Nonlinear Activation Function is used in the operations of Spatial Scaling and *Value* Nonlinear Transformation Adjustment, which is to activate more useful features for better performance. Note that different activation functions may affect the model performance.

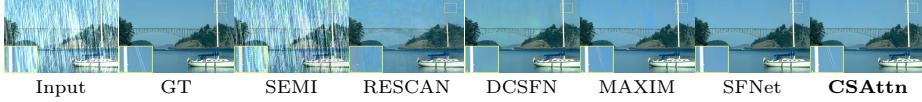
(e) Intra Attention Aggregation. We aggregate these three attention outputs in the final to help the model learn attention features from different levels.

(f) Intra Progressive More Heads. Instead of using the same number of heads from the first attention and the third attention, we suggest using progressive more heads to help the model learn different attention with different levels, which implicitly improves the attention representation to further enhance restoration quality.

(g) Intra Residual Connections. The intra residual connection is introduced to ease the learning for the second and third attention to provide more useful features for the next attention computation.

Table 1: Image deraining results. Our **CSAttn** advances the recent 13 state-of-the-arts on average by at least 0.41 dB PSNR.

Method	Test100		Rain100H		Rain100L		Test2800		Average	
	PSNR \uparrow	SSIM \uparrow	PSNR \uparrow	SSIM \uparrow	PSNR \uparrow	SSIM \uparrow	PSNR \uparrow	SSIM \uparrow	PSNR \uparrow	SSIM \uparrow
DerainNet [16]	22.77	0.810	14.92	0.592	27.03	0.884	24.31	0.861	22.26	0.787
SEMI [66]	22.35	0.788	16.56	0.486	25.03	0.842	24.43	0.782	22.09	0.725
DIDMDN [74]	22.56	0.818	17.35	0.524	25.23	0.741	28.13	0.867	23.32	0.738
UMRL [70]	24.41	0.829	26.01	0.832	29.18	0.923	29.97	0.905	27.39	0.872
RESCAN [36]	25.00	0.835	26.36	0.786	29.80	0.881	31.29	0.904	28.11	0.852
PreNet [52]	24.81	0.851	26.77	0.858	32.44	0.950	31.75	0.916	28.94	0.894
MSPFN [27]	27.50	0.876	28.66	0.860	32.40	0.933	32.82	0.930	30.35	0.900
DCSFN [62]	27.46	0.887	28.98	0.887	34.70	0.961	30.96	0.903	30.53	0.910
MPRNet [73]	30.27	0.897	30.41	0.890	36.40	0.965	33.64	0.938	32.68	0.923
SPAIR [50]	30.35	0.909	30.95	0.892	36.93	0.969	33.34	0.936	32.89	0.927
Uformer [63]	29.17	0.880	30.06	0.884	36.34	0.966	33.36	0.935	32.23	0.916
MAXIM-2S [56]	31.17	0.922	30.81	0.903	38.06	0.977	33.80	0.943	33.46	0.936
SFNet [11]	31.47	0.919	31.90	0.908	38.21	0.974	33.69	0.937	33.81	0.935
CSAttn (Ours)	31.57	0.920	31.62	0.906	39.30	0.979	34.40	0.947	34.22	0.938

**Fig. 3: Image deraining** on Rain100H [68]. Our **CSAttn** is capable of restoring results with finer structures.

4 Experiments

In this section, we evaluate our proposed **CSAttn** for 4 image restoration tasks: (a) image deraining, (b) image desnowing, (c) low-light image enhancement, and (d) real image dehazing. We train separate models for different image restoration tasks.

4.1 Implementation Details

We train **CSAttn** using the AdamW optimizer [43] with the initial learning rate $5e^{-4}$ that is gradually reduced to $1e^{-7}$ with the cosine annealing [42]. The training patch size is set as 256×256 pixels. We replace residual blocks in [11] with our proposed CSAttn blocks, which are set as [6, 6, 12] blocks in 1-3 levels if further mentioned. We use the same loss function in [11] with default parameters to constrain the restored results of **CSAttn** with Ground-Truth.

4.2 Main Results

Results on Image Deraining. Following previous works [11, 27, 50, 73], we evaluate the image deraining task by PSNR/SSIM scores using Y channel in YCbCr color, which is trained on Rain13K dataset and then test on several individual testing datasets. Tab. 1 summarises the quantitative results, where our CSAttn outperforms state-of-the-art approaches when averaged across these 4 datasets, including Test100 [75], Rain100H [69], Rain100L [69], and Test2800 [16]. Compared to the best method SFNet [11], our CSAttn can achieve 0.41 dB improvement on average. Fig. 3 shows that our CSAttn is able to produce clearer images with finer structures, especially in the cropped region.

Table 2: Image desnowing results on CSD (2000) [8], and Snow100K (2000) [53]. Our **CSAttn** achieves the best PSNR and SSIM metrics on image desnowing.

Benchmark	Metrics	DesnowNet [40]	JSTASR [7]	HDCW-Net [8]	TransWeather [57]	MSP-Former [6]	Uformer [64]	Restormer [71]	PromptRestorer [59]	CSAttn Ours
CSD (2000) [8]	PSNR \uparrow	20.13	27.96	29.06	31.76	33.75	33.80	35.43	37.48	37.78
	SSIM \uparrow	0.81	0.88	0.91	0.93	0.96	0.96	0.97	0.99	0.99
Snow100K (2000) [40]	PSNR \uparrow	30.50	23.12	31.54	31.82	33.43	33.81	34.67	36.02	36.08
	SSIM \uparrow	0.94	0.86	0.95	0.95	0.96	0.94	0.95	0.97	0.97



Fig. 4: Image desnowing on CSD (2000) [8]. **CSAttn** is able to recover much cleaner results with fewer artifacts.

Table 3: Low-light image enhancement results on LOL [65]. Our **CSAttn** significantly advances the state-of-the-art approaches by at least 4.22 dB PSNR.

Benchmark	Metrics	Retinex-Net [65]	Zero-DCE [21]	AGLLNet [44]	Zhao et al. [78]	RUAS [38]	SCI [45]	URetinex [67]	UHDFour [34]	CSAttn Ours
LOL [8]	PSNR \uparrow	16.77	16.79	17.52	21.67	16.44	14.78	19.84	23.09	27.31
	SSIM \uparrow	0.54	0.67	0.77	0.87	0.70	0.62	0.87	0.87	0.93



Fig. 5: Low-light image enhancement on LOL [65]. Our **CSAttn** is able to generate results with more natural colors.

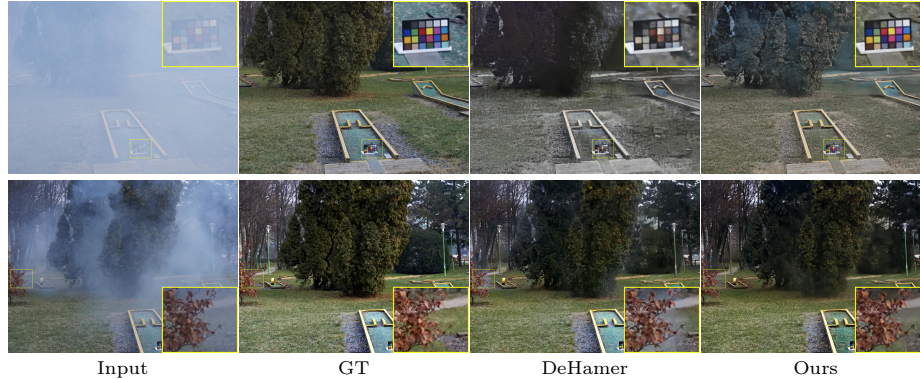
Results on Image Desnowing. We compare our CSAttn on image desnowing task with CNN-based desnowing competitors [7, 8] and Transformer-based approaches [6, 57, 59, 63, 71] on CSD [8] and Snow100K [40] datasets. Moreover, we also compare with Transformer-based general image restoration approaches like Restormer [71], Uformer [63] and PromptRestorer [59]. The results are reported in Tab. 2, where our CSAttn outperforms state-of-the-art approach PromptRestorer [59] on both CSD [8] and Snow100K [40] benchmarks. Fig. 4 shows that our CSAttn removes spatially varying snows while state-of-the-art methods always hand down some artifacts.

Results on Low-light Image Enhancement. We conduct the experiment of low-light image enhancement on widely-used LOL benchmark [65]. Tab. 3 reports the quantitative results. One can obviously observe that our CSAttn achieves 4.22 dB PSNR gains compared to recent works UHDFour [34]. Fig. 5 shows our CSAttn is able to generate more natural results with vivid colors.

Results on Real Image Dehazing. We conduct real image dehazing experiments on real hazy benchmarks: Dense-Haze [1] and NH-Haze [2]. Especially, compared to recent state-of-the-art works PromptRestorer [59], our CSAttn receives 6.03% SSIM on Dense-Haze [1], demonstrating the effectiveness of our CSAttn by achieving significant improvement. Fig. 6 shows our CSAttn is able to generate clearer results with more vivid colors and less haze residuals.

Table 4: Image dehazing results on real benchmarks Dense-Haze [1] and NH-Haze [2]. Our **CSAttn** outperforms recent state-of-the-art method [59].

Benchmark	Metrics	DCP [22]	DehazeNet [5]	AOD [33]	GridNet [39]	FFANet [51]	MSBDN [12]	UHD [79]	DeHamer [20]	PromptRestorer [59]	CSAttn Ours
Dense-Haze [1]	PSNR \uparrow	11.01	9.48	12.82	14.96	12.22	15.13	12.16	16.62	15.86	16.33
	SSIM \uparrow	0.4165	0.4383	0.4683	0.5326	0.4440	0.5551	0.4594	0.5602	0.5680	0.6283
NH-Haze [2]	PSNR \uparrow	12.72	11.76	15.69	18.33	18.13	17.97	16.05	20.66	20.36	20.66
	SSIM \uparrow	0.4419	0.3988	0.5728	0.6667	0.6473	0.6591	0.4612	0.6844	0.7203	0.7209

**Fig. 6: Real image dehazing** on Dense-Haze [1] (**Top**) and NH-Haze [2] (**Bottom**). Our **CSAttn** is capable of recovering results with less haze residuals and more natural colors.

4.3 Ablation Study

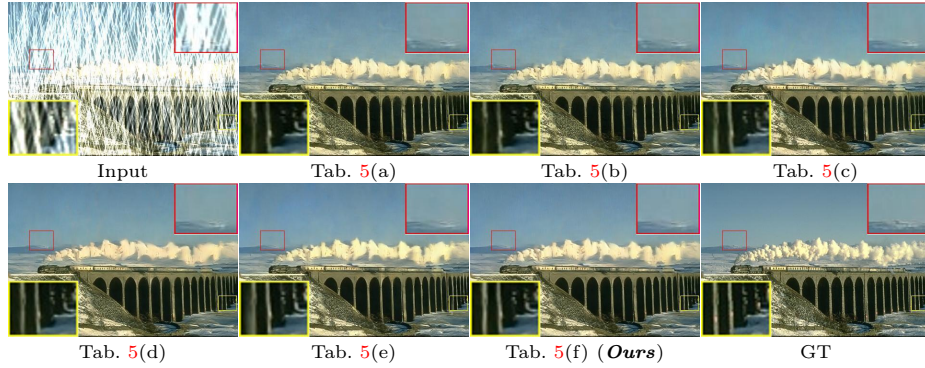
We conduct the ablation study on the Rain100H testing dataset using the model trained on the Rain13K dataset for 100 epochs only. When analyzing our model, the number of blocks is set as [3, 6, 8] from the 1-3 level and the number of channels is set as 32. Next, we describe the influence of each component individually. Tab. 5 and Fig. 7 respectively show the quantitative and qualitative results.

Effect on Nonlinear Activation. As we use the nonlinear activation in the operations of Spatial Scaling and *Value* Nonlinear Transformation Adjustment, analyzing its effectiveness is necessary. Tab. 5 shows that the nonlinear activation function plays a crucial role in image restoration quality (Tab. 5(a) vs. Tab. 5(f)). It can respectively improve PSNR and SSIM by 1.032 dB and 1.58% without consuming additional parameters and FLOPs. Further, we note that most existing attention modules [41, 71] do not utilize nonlinear activation. However, our study clearly suggests that using nonlinear activation in attention is essential, which can learn more representative features for the next attention computation for better performance.

Effect on *Value* Nonlinear Transformation Adjustment. We use *Value* Nonlinear Transformation Adjustment by simply utilizing 1×1 convolution and nonlinear activation to participate in the second and third attention computation. One may wonder to know how it affects the restoration quality. Tab. 5 shows that nonlinear transformation adjustment can improve the PSNR and SSIM by 0.883 dB and 1.77%, respectively (Tab. 5(b) vs. Tab. 5(f)). It indicates that adaptively adjusting the *Value* is able to activate much useful content to

Table 5: Ablation Study. Our full model achieves the best performance in terms of PSNR, SSIM, and MAE.

ID	Experiment	PSNR \uparrow	SSIM \uparrow	MAE \downarrow	FLOPs (G)	Params (M)
(a)	w/o Nonlinear Activation	29.359	0.8765	0.0311	46.110	7.023
(b)	w/o <i>Value</i> Nonlinear Trans. Adj.	29.508	0.8786	0.0306	41.547	6.388
(c)	w/o Intra Attention Aggregation	29.627	0.8805	0.0303	39.265	6.071
(d)	w/o Intra Progressive More Heads	30.101	0.8875	0.0283	46.110	7.023
(e)	w/o Intra Residual Connections	30.189	0.8893	0.0281	46.110	7.023
(f)	Full Model (Ours)	30.391	0.8903	0.0276	46.110	7.023

**Fig. 7: Visual Effect on Each Component.** Our full model is able to produce results with better details and fewer artifacts.

effectively participate in the second and third attention computation for better image restoration.

Effect on Intra Attention Aggregation. We aggregate the output features of all the attention in the final. Tab. 5 shows that our introduced intra feature aggregation respectively improves PSNR, SSIM, and MAE by 0.764 dB, 0.98%, and 0.27% (Tab. 5(c) vs. Tab. 5(f)). The results reveal that aggregating these attention outputs can help the model learn more useful representations with different levels, further improving model performance.

Effect on Intra Progressive More Heads. Instead of using the same number of heads in one CSAtn, we suggest using progressive more heads to improve attention ability. Tab. 5 shows that our introduced progressive more heads respectively improve PSNR, SSIM, and MAE by 0.290 dB, 0.28%, and 0.07% (Tab. 5(d) vs. Tab. 5(f)). The improvement may be because progressive more heads can help the model learn different attention from different levels, which implicitly improves the attention features to further enhance restoration quality.

Effect on Intra Residual Connections. We introduce the intra residual connections into continuous attention designs to ease the learning of difference levels. Tab. 5 shows that the intra residual connections can improve the PSNR by 0.211 dB. By inserting the intra residual connections, our model can provide more useful features into the next attention computation so that it better improves restoration quality.

Effect on Continuous Attention. We introduce a continuous attention learning mechanism to improve the learning ability of attention. In this paper, we

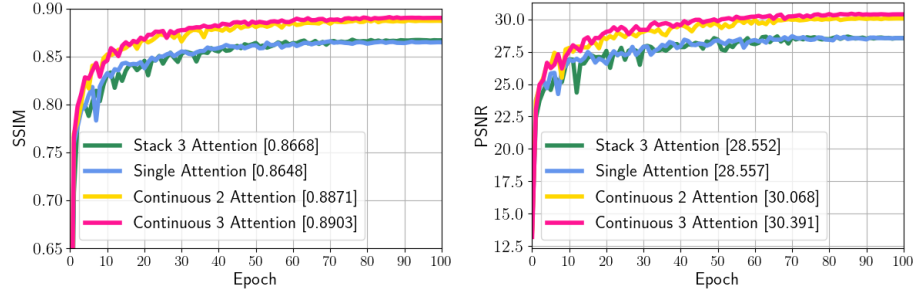


Fig. 8: Learning Curves on Continuous Attention. By plotting the learning curves of single, continuous 2, and continuous 3 attention, we observe that continuous 3 attention outperforms others. The results reveal that performance can be effectively improved by appropriately utilizing attention within a suitable way. Note that single attention means the used attention in Restormer [71].

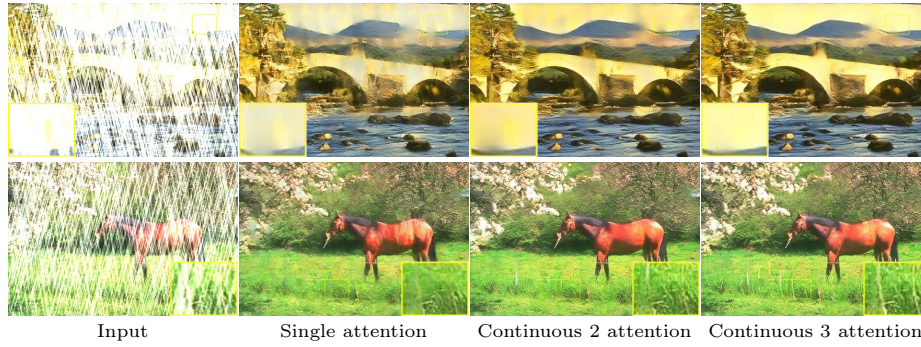


Fig. 9: Visual Effect on Continuous Attention. Our continuous 3 attention is able to generate results with fewer artifacts (**Top**) and finer structures (**Bottom**), while the single attention is not effective in handling such heavy rain, and the continuous 2 attention hands down artifacts and blur textures.

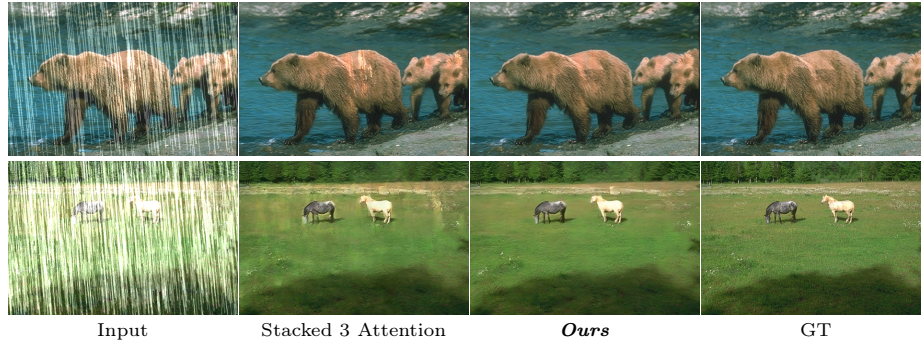


Fig. 10: Visual Effect on Attention Forms. Stacking 3 attention of [71] cannot effectively remove heavy degradation, while our proposed continuous attention form with a series of key designs produces visually pleasing results with fewer artifacts.

use continuous 3 attention to effectively scale up the model capacity. One may wonder how the different number of continuous attentions affects the restora-

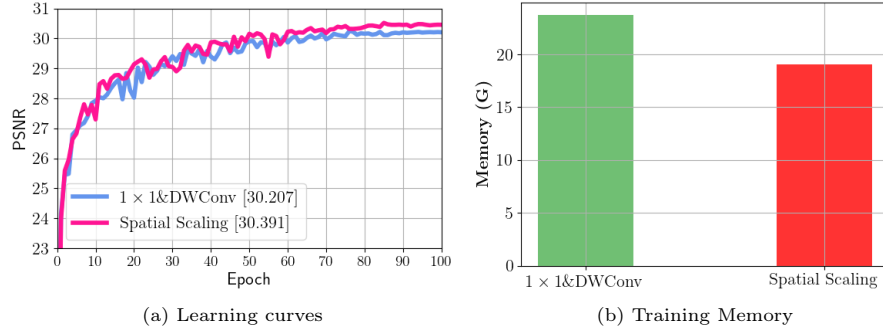


Fig. 11: Learning Curves vs. Training Memory on Spatial Scaling Learning. By continuously scaling the spatial sizes into the smaller, the training budget is saved (b) and the results keep competitive with the model without scaling (a).

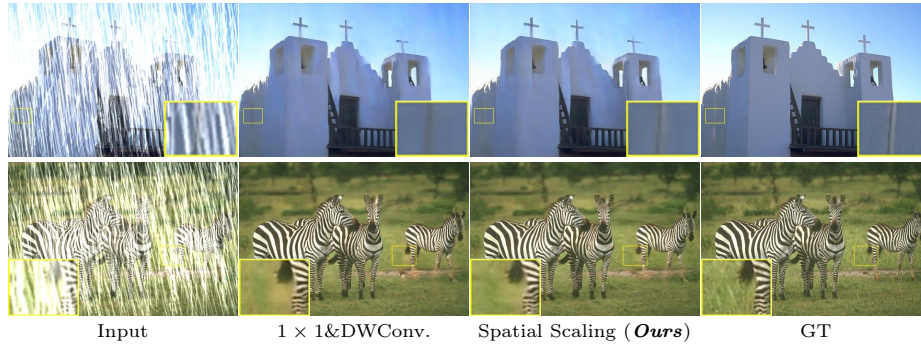


Fig. 12: Visual Effect on Spatial Scaling. Using spatial scaling is able to generate results with sharper structures and fewer artifacts.

tion quality and what the results of 3 attention of [71] are compared with the proposed form. Fig. 8 shows the learning curves of one, continuous two/three attention. We also compare the model with stacked three attention in [71]. We note that continuous 3 attention obviously outperforms both 1 attention and continuous 2 attention, which suggests using continuous 3 attention makes attention empower stronger representative learning ability. Moreover, stacking 3 attention of [71] cannot achieve high-quality restoration results, which further indicates simple cascaded attention is not as good as our designed module. Fig. 9 presents a visual example of continuous attention with different orders, where our continuous 3 attention is able to generate results with less rainy residuals and finer structures. Fig. 10 shows that stacked three attention hands down extensive rain traces or artifacts, while our proposed method generates much clearer results.

Effect on Spatial Scaling. We propose spatial scaling to save the training budget while keeping superior performance compared with the model without using scaling. Hence, one may be interested in how it affects the results compared model without using spatial scaling. To answer this question, we compare with the model using 1×1 convolution and 3×3 depth-wise convolution which are the same operations with the first attention. The learning curves are shown in

Table 6: Effect on Nonlinear Activation Functions. Compared with ReLU [18], LeakyReLU [46], and SiLU [15], GELU [24] achieves the best performance in terms of PSNR, SSIM, and MAE. The PSNR can be improved as large as 0.136dB, compared with ReLU activation.

ID	Activation	PSNR \uparrow	SSIM \uparrow	MAE \downarrow	FLOPs (G) \downarrow	Params (M) \downarrow
(a)	ReLU [18]	30.255	0.8882	0.0280	46.110	7.023
(b)	LeakyReLU [46]	30.276	0.8877	0.0279	46.110	7.023
(c)	SiLU [15]	30.286	0.8897	0.0279	46.110	7.023
(d)	GELU [24] (Default)	30.391	0.8903	0.0276	46.110	7.023

Table 7: Comparisons on Model Sizes and Computational Complexity. Our **CSAttn** has competitive model sizes and computational complexity compared with state-of-the-art CNN-based methods [11] and Transformer-based approaches [59, 63, 71] and Transformer-CNN fusion techniques [20].

Method	Restormer [71]	Uformer [63]	DeHamer [20]	SFNet [11]	PromptRestorer [59]	CSAttn <i>Ours</i>
Params (M) \downarrow	26.1	20.63	132.5	13.3	24.4	21.75
FLOPs (G) \downarrow	141.0	41.55	59.3	125.4	186.3	137.71

Fig. 11(a) and the training memory is illustrated in Fig. 11(b). One can observe that the results of using spatial scaling are better than the model without scaling while consuming less training memory. Fig. 12 shows that using spatial scaling is capable of producing results with sharper structures and fewer artifacts.

Effect on Nonlinear Activation Functions. Tab. 6 further summarises the results of different nonlinear activation functions. We note that the GELU activation is the best in terms of PSNR, SSIM, and MAE. Compared with other activation functions, the PSNR can be improved as large as 0.136 dB.

4.4 Model Sizes and Computational Complexity

We further report the comparisons of model sizes and computational complexity in Tab. 7. As can be seen, our **CSAttn** consumes comparable model parameters and FLOPs compared with previous state-of-the-art CNN-based methods and Transformer-based approaches, further demonstrating that the performance improvement is not from the big model sizes.

5 Concluding Remarks

We have explored the potential of attention for image restoration by proposing a simple and effective Continuous Scaling Attention (**CSAttn**). By introducing various design components, we have demonstrated the strong learning ability of attention without using feed-forward networks which are necessary in existing Transformer frameworks. We have analyzed the effectiveness of each component and revealed its role in our CSAttn. We have conducted extensive experiments and showed that our CSAttn outperforms state-of-the-art CNN-based and Transformer-based image restoration approaches on various applications, including deraining, desnowing, low-light enhancement, and real dehazing.

References

1. Ancuti, C.O., Ancuti, C., Sbert, M., Timofte, R.: Dense-haze: A benchmark for image dehazing with dense-haze and haze-free images. In: ICIP. pp. 1014–1018 (2019) [9](#), [10](#)
2. Ancuti, C.O., Ancuti, C., Timofte, R.: Nh-haze: An image dehazing benchmark with non-homogeneous hazy and haze-free images. In: CVPR workshops. pp. 444–445 (2020) [9](#), [10](#)
3. Anwar, S., Khan, S., Barnes, N.: A deep journey into super-resolution: A survey. ACM Computing Surveys (2019) [4](#)
4. Ba, J.L., Kiros, J.R., Hinton, G.E.: Layer normalization. arXiv:1607.06450 (2016) [6](#)
5. Cai, B., Xu, X., Jia, K., Qing, C., Tao, D.: Dehazenet: An end-to-end system for single image haze removal. IEEE TIP (2016) [10](#)
6. Chen, S., Ye, T., Liu, Y., Liao, T., Ye, Y., Chen, E.: Msp-former: Multi-scale projection transformer for single image desnowing. arXiv preprint arXiv:2207.05621 (2022) [2](#), [4](#), [9](#)
7. Chen, W.T., Fang, H.Y., Ding, J.J., Tsai, C.C., Kuo, S.Y.: Jstasr: Joint size and transparency-aware snow removal algorithm based on modified partial convolution and veiling effect removal. In: ECCV. pp. 754–770 (2020) [9](#)
8. Chen, W.T., Fang, H.Y., Hsieh, C.L., Tsai, C.C., Chen, I., Ding, J.J., Kuo, S.Y., et al.: All snow removed: Single image desnowing algorithm using hierarchical dual-tree complex wavelet representation and contradict channel loss. In: ICCV. pp. 4196–4205 (2021) [9](#)
9. Cho, S.J., Ji, S.W., Hong, J.P., Jung, S.W., Ko, S.J.: Rethinking coarse-to-fine approach in single image deblurring. In: ICCV (2021) [4](#), [5](#)
10. Cui, X., Wang, C., Ren, D., Chen, Y., Zhu, P.: Semi-supervised image deraining using knowledge distillation. IEEE TCSVT **32**(12), 8327–8341 (2022) [3](#)
11. Cui, Y., Tao, Y., Bing, Z., Ren, W., Gao, X., Cao, X., Huang, K., Knoll, A.: Selective frequency network for image restoration. In: ICLR (2023) [4](#), [5](#), [8](#), [14](#)
12. Dong, H., Pan, J., Xiang, L., Hu, Z., Zhang, X., Wang, F., Yang, M.H.: Multi-scale boosted dehazing network with dense feature fusion. In: CVPR (2020) [10](#)
13. Dosovitskiy, A., Beyer, L., Kolesnikov, A., Weissenborn, D., Zhai, X., Unterthiner, T., Dehghani, M., Minderer, M., Heigold, G., Gelly, S., et al.: An image is worth 16x16 words: Transformers for image recognition at scale. In: ICLR (2021) [2](#), [4](#), [5](#)
14. Dudhane, A., Zamir, S.W., Khan, S., Khan, F., Yang, M.H.: Burst image restoration and enhancement. In: CVPR (2022) [3](#)
15. Elfving, S., Uchibe, E., Doya, K.: Sigmoid-weighted linear units for neural network function approximation in reinforcement learning. Neural networks **107**, 3–11 (2018) [14](#)
16. Fu, X., Huang, J., Ding, X., Liao, Y., Paisley, J.: Clearing the skies: A deep network architecture for single-image rain removal. TIP (2017) [8](#)
17. Geva, M., Schuster, R., Berant, J., Levy, O.: Transformer feed-forward layers are key-value memories. In: EMNLP (2021) [1](#), [2](#), [7](#)
18. Glorot, X., Bordes, A., Bengio, Y.: Deep sparse rectifier neural networks. In: AIS-TATS. pp. 315–323 (2011) [14](#)
19. Goodfellow, I.J., Pouget-Abadie, J., Mirza, M., Xu, B., Warde-Farley, D., Ozair, S., Courville, A.C., Bengio, Y.: Generative adversarial nets. In: NeurIPS. pp. 2672–2680 (2014) [4](#)

20. Guo, C.L., Yan, Q., Anwar, S., Cong, R., Ren, W., Li, C.: Image dehazing transformer with transmission-aware 3d position embedding. In: CVPR. pp. 5812–5820 (2022) [2](#), [4](#), [10](#), [14](#)
21. Guo, C., Li, C., Guo, J., Loy, C.C., Hou, J., Kwong, S., Cong, R.: Zero-reference deep curve estimation for low-light image enhancement. In: CVPR. pp. 1777–1786 (2020) [9](#)
22. He, K., Sun, J., Tang, X.: Single image haze removal using dark channel prior. TPAMI (2010) [1](#), [10](#)
23. He, K., Zhang, X., Ren, S., Sun, J.: Deep residual learning for image recognition. In: CVPR (2016) [2](#)
24. Hendrycks, D., Gimpel, K.: Gaussian error linear units (gelus). arXiv preprint arXiv:1606.08415 (2016) [14](#)
25. Hu, J., Shen, L., Albanie, S., Sun, G., Wu, E.: Squeeze-and-excitation networks. IEEE TPAMI (2019) [2](#)
26. Huang, J.B., Singh, A., Ahuja, N.: Single image super-resolution from transformed self-exemplars. In: CVPR (2015) [1](#)
27. Jiang, K., Wang, Z., Yi, P., Huang, B., Luo, Y., Ma, J., Jiang, J.: Multi-scale progressive fusion network for single image deraining. In: CVPR (2020) [8](#)
28. Khan, S., Naseer, M., Hayat, M., Zamir, S.W., Khan, F.S., Shah, M.: Transformers in vision: A survey. arXiv:2101.01169 (2021) [2](#), [4](#)
29. Kong, L., Dong, J., Ge, J., Li, M., Pan, J.: Efficient frequency domain-based transformers for high-quality image deblurring. In: CVPR. pp. 5886–5895 (2023) [2](#), [4](#)
30. Krizhevsky, A., Sutskever, I., Hinton, G.E.: Imagenet classification with deep convolutional neural networks. In: NIPS (2012) [2](#)
31. Ledig, C., Theis, L., Huszár, F., Caballero, J., Cunningham, A., Acosta, A., Aitken, A., Tejani, A., Totz, J., Wang, Z., et al.: Photo-realistic single image super-resolution using a generative adversarial network. In: CVPR (2017) [2](#)
32. Ledig, C., Theis, L., Huszar, F., Caballero, J., Cunningham, A., Acosta, A., Aitken, A.P., Tejani, A., Totz, J., Wang, Z., Shi, W.: Photo-realistic single image super-resolution using a generative adversarial network. In: CVPR. pp. 105–114 (2017) [4](#)
33. Li, B., Peng, X., Wang, Z., Xu, J., Feng, D.: Aod-net: All-in-one dehazing network. In: ICCV (2017) [2](#), [10](#)
34. Li, C., Guo, C.L., Zhou, M., Liang, Z., Zhou, S., Feng, R., Loy, C.C.: Embedding fourier for ultra-high-definition low-light image enhancement. In: ICLR (2023) [9](#)
35. Li, S., Araujo, I.B., Ren, W., Wang, Z., Tokuda, E.K., Junior, R.H., Cesar-Junior, R., Zhang, J., Guo, X., Cao, X.: Single image deraining: A comprehensive benchmark analysis. In: CVPR (2019) [4](#)
36. Li, X., Wu, J., Lin, Z., Liu, H., Zha, H.: Recurrent squeeze-and-excitation context aggregation net for single image deraining. In: ECCV (2018) [8](#)
37. Liang, J., Cao, J., Sun, G., Zhang, K., Van Gool, L., Timofte, R.: SwinIR: Image restoration using swin transformer. In: ICCV Workshops (2021) [2](#), [4](#)
38. Liu, R., Ma, L., Zhang, J., Fan, X., Luo, Z.: Retinex-inspired unrolling with cooperative prior architecture search for low-light image enhancement. In: CVPR. pp. 10561–10570 (2021) [9](#)
39. Liu, X., Ma, Y., Shi, Z., Chen, J.: Griddehazenet: Attention-based multi-scale network for image dehazing. In: ICCV (2019) [10](#)
40. Liu, Y.F., Jaw, D.W., Huang, S.C., Hwang, J.N.: Desnownet: Context-aware deep network for snow removal. TIP **27**(6), 3064–3073 (2018) [2](#), [9](#)

41. Liu, Z., Lin, Y., Cao, Y., Hu, H., Wei, Y., Zhang, Z., Lin, S., Guo, B.: Swin transformer: Hierarchical vision transformer using shifted windows. In: ICCV (2021) [3](#), [4](#), [10](#)
42. Loshchilov, I., Hutter, F.: SGDR: Stochastic gradient descent with warm restarts. In: ICLR (2017) [8](#)
43. Loshchilov, I., Hutter, F.: Decoupled weight decay regularization. In: ICLR (2019) [8](#)
44. Lv, F., Li, Y., Lu, F.: Attention guided low-light image enhancement with a large scale low-light simulation dataset. IJCV **129**(7), 2175–2193 (2021) [9](#)
45. Ma, L., Ma, T., Liu, R., Fan, X., Luo, Z.: Toward fast, flexible, and robust low-light image enhancement. In: CVPR. pp. 5637–5646 (2022) [9](#)
46. Maas, A.L., Hannun, A.Y., Ng, A.Y., et al.: Rectifier nonlinearities improve neural network acoustic models. In: ICML. vol. 30, p. 3 (2013) [14](#)
47. Pan, J., Hu, Z., Su, Z., Yang, M.H.: l_0 -regularized intensity and gradient prior for deblurring text images and beyond. TPAMI **39**(2), 342–355 (2017) [1](#)
48. Pan, J., Liu, S., Sun, D., Zhang, J., Liu, Y., Ren, J.S.J., Li, Z., Tang, J., Lu, H., Tai, Y., Yang, M.: Learning dual convolutional neural networks for low-level vision. In: CVPR. pp. 3070–3079 (2018) [4](#)
49. Pan, J., Sun, D., Pfister, H., Yang, M.H.: Blind image deblurring using dark channel prior. In: CVPR (2016) [1](#)
50. Purohit, K., Suin, M., Rajagopalan, A., Boddeti, V.N.: Spatially-adaptive image restoration using distortion-guided networks. In: ICCV (2021) [8](#)
51. Qin, X., Wang, Z., Bai, Y., Xie, X., Jia, H.: Ffa-net: Feature fusion attention network for single image dehazing. In: AAAI. vol. 34, pp. 11908–11915 (2020) [10](#)
52. Ren, D., Zuo, W., Hu, Q., Zhu, P., Meng, D.: Progressive image deraining networks: A better and simpler baseline. In: CVPR (2019) [2](#), [8](#)
53. Rim, J., Lee, H., Won, J., Cho, S.: Real-world blur dataset for learning and benchmarking deblurring algorithms. In: ECCV (2020) [9](#)
54. Simonyan, K., Zisserman, A.: Very deep convolutional networks for large-scale image recognition. In: ICLR (2015) [2](#)
55. Tsai, F.J., Peng, Y.T., Lin, Y.Y., Tsai, C.C., Lin, C.W.: Stripformer: Strip transformer for fast image deblurring. In: ECCV (2022) [2](#), [4](#)
56. Tu, Z., Talebi, H., Zhang, H., Yang, F., Milanfar, P., Bovik, A., Li, Y.: Maxim: Multi-axis mlp for image processing. In: CVPR. pp. 5769–5780 (2022) [8](#)
57. Valanarasu, J.M.J., Yasarla, R., Patel, V.M.: Transweather: Transformer-based restoration of images degraded by adverse weather conditions. In: CVPR. pp. 2353–2363 (2022) [9](#)
58. Wang, C., Pan, J., Lin, W., Dong, J., Wu, X.M.: Selfpromer: Self-prompt dehazing transformers with depth-consistency. arXiv preprint arXiv:2303.07033 (2023) [2](#)
59. Wang, C., Pan, J., Wang, W., Dong, J., Wang, M., Ju, Y., Chen, J.: Promptrestorer: A prompting image restoration method with degradation perception. In: NeurIPS (2023) [9](#), [10](#), [14](#)
60. Wang, C., Pan, J., Wu, X.: Online-updated high-order collaborative networks for single image deraining. In: AAAI. pp. 2406–2413 (2022) [2](#)
61. Wang, C., Wu, Y., Su, Z., Chen, J.: Joint self-attention and scale-aggregation for self-calibrated deraining network. In: ACM MM (2020) [2](#)
62. Wang, C., Xing, X., Wu, Y., Su, Z., Chen, J.: DCSFN: deep cross-scale fusion network for single image rain removal. In: ACM MM. pp. 1643–1651 (2020) [2](#), [8](#)
63. Wang, Z., Cun, X., Bao, J., Liu, J.: Uformer: A general u-shaped transformer for image restoration. arXiv:2106.03106 (2021) [2](#), [4](#), [5](#), [8](#), [9](#), [14](#)

64. Wang, Z., Cun, X., Bao, J., Zhou, W., Liu, J., Li, H.: Uformer: A general u-shaped transformer for image restoration. In: CVPR. pp. 17683–17693 (2022) [9](#)
65. Wei, C., Wang, W., Yang, W., Liu, J.: Deep retinex decomposition for low-light enhancement. In: BMVC. p. 155 (2018) [9](#)
66. Wei, W., Meng, D., Zhao, Q., Xu, Z., Wu, Y.: Semi-supervised transfer learning for image rain removal. In: CVPR (2019) [8](#)
67. Wu, W., Weng, J., Zhang, P., Wang, X., Yang, W., Jiang, J.: Uretinex-net: Retinex-based deep unfolding network for low-light image enhancement. In: CVPR. pp. 5901–5910 (2022) [9](#)
68. Yang, W., Tan, R.T., Feng, J., Liu, J., Guo, Z., Yan, S.: Deep joint rain detection and removal from a single image. In: CVPR (2017) [8](#)
69. Yang, W., Tan, R.T., Feng, J., Liu, J., Guo, Z., Yan, S.: Deep joint rain detection and removal from a single image. In: CVPR (2017) [8](#)
70. Yasarla, R., Patel, V.M.: Uncertainty guided multi-scale residual learning-using a cycle spinning cnn for single image de-raining. In: CVPR (2019) [8](#)
71. Zamir, S.W., Arora, A., Khan, S., Hayat, M., Khan, F.S., Yang, M.H.: Restormer: Efficient transformer for high-resolution image restoration. In: CVPR. pp. 5718–5729 (2022) [2](#), [3](#), [4](#), [5](#), [9](#), [10](#), [12](#), [13](#), [14](#)
72. Zamir, S.W., Arora, A., Khan, S., Hayat, M., Khan, F.S., Yang, M.H., Shao, L.: Learning enriched features for real image restoration and enhancement. In: ECCV (2020) [3](#)
73. Zamir, S.W., Arora, A., Khan, S., Hayat, M., Khan, F.S., Yang, M.H., Shao, L.: Multi-stage progressive image restoration. In: CVPR (2021) [3](#), [4](#), [8](#)
74. Zhang, H., Patel, V.M.: Density-aware single image de-raining using a multi-stream dense network. In: CVPR (2018) [8](#)
75. Zhang, H., Sindagi, V., Patel, V.M.: Image de-raining using a conditional generative adversarial network. TCSVT (2019) [8](#)
76. Zhang, K., Zuo, W., Chen, Y., Meng, D., Zhang, L.: Beyond a gaussian denoiser: Residual learning of deep cnn for image denoising. TIP (2017) [4](#)
77. Zhang, Y., Tian, Y., Kong, Y., Zhong, B., Fu, Y.: Residual dense network for image restoration. TPAMI (2020) [2](#)
78. Zhao, L., Lu, S., Chen, T., Yang, Z., Shamir, A.: Deep symmetric network for underexposed image enhancement with recurrent attentional learning. In: ICCV. pp. 12055–12064 (2021) [9](#)
79. Zheng, Z., Ren, W., Cao, X., Hu, X., Wang, T., Song, F., Jia, X.: Ultra-high-definition image dehazing via multi-guided bilateral learning. In: CVPR. pp. 16185–16194 (2021) [10](#)
80. Zhu, H., Wang, C., Zhang, Y., Su, Z., Zhao, G.: Physical model guided deep image deraining. In: ICME. pp. 1–6 (2020) [3](#)